The ALTCRISS project on board the International Space Station

M. Casolino [a,*], F. Altamura [a], M. Minori [a], P. Picozza [a], C. Fuglesang [b], A. Galper [c], A. Popov [c], V. Benghin [d], V. M. Petrov [d], A. Nagamatsu [e], T. Berger [f], G. Reitz [f], M. Durante [g], M. Pugliese [g], V. Roca [g], F. Cucinotta [h], E. Semones [h], M. Shavers [i], V. Guarnieri [j], C. Lobascio [j]

[a] *INFN and University of Rome Tor Vergata, Department of Physics, Via della Ricerca Scientifica 1, 00133 Rome, Italy*

[b] *European Astronaut Centre, ESA, Cologne*

[c] *Moscow State Engineering Physics Institute, Moscow, Russia*

[d] *Institute for Biomedical Problems, Moscow, Russia*

[e] *Japan Aerospace Exploration Agency, Japan*

[f] *DLR, Aerospace Medicine, Radiation Biology, Koln, Germany*

[g] *University Federico II, and INFN Napoli, Italy*

[h] *National Aeronautics and Space Administration, Lyndon B Johnson Space Centre, Houston, TX, USA*

[i] *Radiation Biophysics Laboratory, Wyle Laboratories, Houston, TX, USA*

[j] *Alcatel Alenia Space Torino, Italy*

Abstract

The Altcriss project aims to perform a long term survey of the radiation environment on board the International Space Station. Measurements are being performed with active and passive devices in different locations and orientations of the Russian segment of the station. The goal is perform a detailed evaluation of the differences in particle fluence and nuclear composition due to different shielding material and attitude of the station. The Sileye-3/Alteino detector is used to identify nuclei up to

Iron in the energy range above $\simeq$ 60 MeV/n; a number of passive dosimeters (TLDs, CR39) are also placed in the same location of Sileye-3 detector. Polyethylene shielding is periodically interposed in front of the detectors to evaluate the effectiveness of shielding on the nuclear component of the cosmic radiation. The project was submitted to ESA in reply to the AO the Life and Physical Science of 2004 and was begun in December 2005. Dosimeters and data cards are rotated every six months: up to now three launches of dosimeters and data cards have been performed and have been returned with the end expedition 12 and 13.

Key words: Cosmic Rays, Nuclear Abundances, International Space Station
PACS: 96.40-z, 95.55-n

---

1 Introduction

The International Space Station is an unique testbed for long term human permanence in space and a proving ground for future missions to the Moon and Mars. Indeed it is expected that human presence in space will increase both in the number of space travellers and the duration of the missions(1; 2; 3). Therefore a detailed knowledge of the radiation field in space, its effects on human physiology and the associated risk have been and will be needed in mission planning. In addition to a detailed understanding of the biological effects on the human body(4), this task requires precise measurements of the particles in the cosmic ray environment, their temporal variations due to solar modulation or Solar Particle Events and their orbital dependence (due to geomagnetic cutoff and trapped particles encountered in the South Atlantic Anomaly) as well as to how these particles interact with the hull of the station. Nuclear abundances and differential spectra of cosmic ray nuclei have been studied over a wide energy range and in different points of the Heliosphere by a number of spacecrafts (ACE, Sampex, Ulysses). This has greatly advanced the knowledge of the cosmic ray composition and the physical phenomena involved such as solar modulation, solar energetic particles, trapping of particles in the radiation belts and so on. Cosmic rays, consisting of 99% H and He ions and 1% heavier nuclei (which - however - represent the dominant component of the equivalent dose(5)) interact with the spacecraft material, producing secondary particles that result in modified nuclear abundances and energy spectrum. For these reasons the radiation environment on board the ISS is being monitored by a number of different detectors employing different techniques(6; 7; 8; 9; 10; 11; 12; 13). Due to the large inhomogeneity in the hull of the station, it is still an open question to assess *a priori* the

* Corresponding author.
Email address: casolino@roma2.infn.it (M. Casolino).

cosmic ray flux and the corresponding dose rate in the different points of the station(15; 14; 16; 17). Furthermore, to these uncertainties add the effects of densely ionizing field on the human body, such as the accurate estimation of the damage to cells and the associated risk induced by heavily charged radiation on astronauts(18; 19; 20). Radiation evaluation and protection in space is therefore an interdisciplinary field, involving scientists from many fields, such as cosmic ray physics, radiobiology, dosimetry and computer science.

2 The Altcriss project

The Altcriss (Alteino Long Term Monitoring of Cosmic Rays on the International Space Station) project aims to perform a long term survey of the radiation and cosmic ray environment on board the ISS. Is was submitted to ESA in response to the AO in Life and Physical Science of 2004 with observations beginning at the end of 2005 (increment 12) and expected to continue for three years. This experiment follows previous ones on Mir where relative nuclear abundances and Light Flash perception(21; 22; 23) measurements have been performed with similar silicon detector based device (Sileye-1 and Sileye-2). Previous measurements on ISS with Silye-3/Alteino have been performed in 2002 and 2005 in the framework of the first and second Italian-Soyuz Missions. In those missions measurements were limited to the taxi flight duration (< 10 days each) and to the Pirs module. The main goals of the project are:

- *Monitoring of long and short term solar modulation of cosmic rays.* The active nature of the device allows to identify particles of galactic, trapped and solar origin according to their position and temporal profile. Observations are currently being carried at solar minimum, going toward solar maximum.
- *Observations of Solar Particle Events.* We expect in three years(24) about 10 events with an energy and fluence high enough to be reach the interior of the station and trigger our detector. For these events we plan to observe the temporal profile and the nuclear abundances.
- *Survey of different locations of the ISS modules.* By relocating and rotating the instrument it is possible to study the differences in flux and nature of cosmic rays due to the different shielding of the station material (hull, racks, instruments etc.). Flux is also dependent on station attitude and orientation: currently several locations in the Pirs (Russian docking) and in the Service Modules (Central area, crew cabins) have been studied. In the future it is planned to make measurements in the Columbus module and in the US section of the station.
- *Study of the effectiveness of shielding materials.* Different materials are being considered to reduce the dose to the astronauts: the current approach in weight effective shielding in space is to use low Z materials for their higher stopping power and fragmentation cross-section of the projectile. In this way

it is possible to reduce the LET (Linear Energy Transfer) and the quality factor of the radiation, thus reducing the equivalent dose to the astronauts. Although several steps are being taken in this direction (such as putting water reserves in the crew quarters) the best materials from this standpoint are often not practical. For instance, liquid hydrogen would be the best shielding material but cannot be used for the dangers involved in handling such a material. In the Altcriss project we are currently employing two set of tiles to study the effect of shielding on the nuclear radiation field:

(1) Polyethylene tiles. These are similar to what currently used in the crew cabin of US section of the ISS. These tiles are located on top and bottom of the bidirectional acceptance window of the detector to evaluate the effect of this material (for a thickness of $\simeq 5g/cm^2$) on the radiation and the nuclear abundances. Passive dosimeters are interposed between the detector and the shielding tile to compare the dose measured with TLD and CR-39 with active data coming from Sileye-3/Alteino.

(2) Multimaterial tiles. These tiles are divided into four sections, each composed of a different material: Polyethylene, Kevlar, Nextel/Capton Composite and one section left empty as a reference. These tiles were used in 2005 in the framework of the second Italian Soyuz Mission. In the Altcriss project they have until now being used with passive dosimeters interposed between the shielding tiles to measure the radiation dose.

- *Comparison with other detectors.* Given the complexity of the radiation field in space, in order to build a comprehensive picture of the cosmic ray environment on board the ISS it is necessary to correlate the measurements obtained with Sileye-3/Alteino with other detectors on board the station. To this purpose the device was located in the starboard cabin close to Matroska-R spherical phantom. Furthermore a cross-comparison measurement campain with ESA Matroska facility is planned to be carried forth during expedition 15: in this case Sileye-3 will be placed at the same locations of the human phantom (but not at the same time) to have the exact comparison of the cosmic ray flux. Comparison of the nuclear abundances measured with NASA IV-CPDS will also be performed. To study the propagation of cosmic ray from the exterior to the interior of the station the data coming from the Pamela experiment, a satellite borne cosmic ray detector placed in a 350*650 km, 70^o inclination will be used.

3 Sileye-3/Alteino characteristics

Sileye-3 is a cosmic-ray detector (27; 28; 29) composed of 8 silicon strip detector planes, each divided in 32 strips, with 2.5 mm pitch. There are 4 planes oriented along the X view and 4 planes along the Y view. The general scheme of the detector is shown in Figure 1. Two scintillators (1 mm thick each) are

located on top and bottom of the silicon stack to provide the trigger. The scintillators are covered by a $50\mu m$ Mylar foil located at 12.5 mm from the scintillator, and an Al (70 μm) and Mylar ($50\mu m$) foil at distance 12.5 mm from the mylar plane.

Each Silicon plane has a size of 8 cm * 8 cm, with a thickness of $380\mu m$; interplanar distance is 1.5 cm (except between planes 4 and 5 where is 2.5cm), resulting in a geometric factor of 23.78 $cm^2 sr$ (considering that particles from both sides can trigger the detector). The front-end electronics is based on a VLSI ASIC, the CR1.4P chip (26) originally developed for the Silicon-Tungsten calorimeter of the magnetic spectrometer PAMELA (25), a satellite-borne apparatus for the study of antimatter component of cosmic rays. This chip has a dynamic range of 1600 minimum ionizing particles (MIP) [1], with good noise performance ($\simeq 2700\ e^-$ rms + $5\ e^-/pF$) and low power consumption ($< 100mW/chip$). Characteristics are summarized in Table 10. Each circuit has 16 channels, composed of a charge sensitive preamplifier, a shaping amplifier, a track-and-hold circuit and an output multiplexer. Over the whole range the maximum deviation from linearity is $< 2.5\%$ with an average linearity better than 1%. Outputs are connected to a 16-bit ADC (with serial digital output) through an analogue multiplexer and an operational amplifier. Two CR1 chips are present on each front-end board to read the 32 strips of the silicon plane. A custom Read Out Board performs the tasks of trigger handling and data acquisition. It can be divided in two sections: The Front-end interface logic and the DSP. The Read-out section, based on a Quicklogic fuse programmable logic, includes 8 16-bit shift registers to parallelize serial data coming from ADCs (Analog to Digital Conversion), 3 32-bit counters for the Scintillators (single counters and coincidence signal), a programmable delay generator, 16 inputs for temperature alarms with interrupt generator and a 16-bit parallel bus for communication with the DSP. The DSP section is based on the ADSP-2181, a 16-bit integer processor, used for pedestal subtraction and data compression.
The trigger is defined with the logical AND of the signals of the two scintillators $S1$ and $S2$. The trigger gives the hold signal to the preamplifiers (peaked at $1\mu s$) and begins the multiplexed acquisition of the 256 channels and their analog to digital conversion. The DSP then performs data reduction, consisting in the removal of all strips not crossed by particles. Data are then stored in a temporary buffer to be sent via an ISA interface to a storage and data handling computer, a PC-104 board based on an AMD586 100 Mhz. A quartz clock is used to save event time; the beginning time of each session is written to synchronize (in the off-line stage) the station time with the event time.

[1] 1 MIP is defined as the energy lost by minimum ionizing protons (2 GeV). In our case we have 1 MIP=5.1 fC in 380 μm thick detectors).

4 Data acquisition

Each session begins with the calibration of the silicon strips of the detector. This consists in the acquisition of 1024 pedestal events and the calculation of the pedestal average P_i and rms σ_i for each strip i. Thresholds T_i are set according to the formula $T_i = P_i + n\sigma_i$, with $n = 1$. The raw event, consisting in a 512 byte (256 channels * 2 byte/channel) matrix, is reduced by pedestal suppression with the removal of all strips with values below the threshold T_i. The choice of $n = 1$ (one rms) was used as a suitable compromise between data compression and strip hit lost to pedestal drift due to temperature effects between calibrations [2]. Temperature drift, non negligible before thermal equilibrium in the device is reached (several hours after turn on), influences pedestal position; to compensate for this effect calibrations are repeated every 120 seconds. This effect does not affect detector noise: the rms of the 256 detector strips at the beginning and at the end of the mission shows that average pedestal rms is below 7 channels for the whole duration of the acquisition (only one strip - not shown in the Figure - has a rms of 2000). Each calibration takes 2 seconds, after which particle acquisition is resumed. Each event also includes the value of three scintillator counters (S1, S2 , S1*S2) and the internal DSP clock, to synchronize it with the PC-104 clock. All events are stored in one of the two DSP buffers (15 kbyte each); when one buffer is filled the PC-104 begins data transfer while the second buffer is being filled. This procedure allows asynchronous data readout through the ISA bus and reduction of the dead time due to data transfer. The device has been tested on accelerator in Uppsala (TSL laboratory) with low energy ($\simeq 45 MeV/n$ D, C, O) and Dubna (200 MeV/n He).

5 Passive Dosimeters

A number of passive dosimeters is used to measure the dose absorbed in space in the shielded and unshielded configuration and complement the active data coming from Sileye-3. These dosimeters come from JAXA, DLR and Napoli Federico II University and consist of different types of TLD and CR39 detectors. They are placed in four pouches:

- two pouches with all dosimeters are interposed between the two polyethylene shielding tiles and the acceptance windows of Sileye-3 when performing mea-

[2] A charge inject procedure is also performed in the calibration procedure. However this charge is injected applying the same voltage to input capacitors present on each channel. The difference in capacitance of between capacitors is about 10%: for this reason it is more accurate to calibrate the detector directly using cosmic rays.

surements in the shielded configuration (and thus are shielded by roughly 2π polyethylene). When the Silicon detector is performing unshielded measurements the tiles and pouches are packed close one to the other and placed near the device (and the dosimeters are behind 4π polyethylene shielding).
- one pouch with four Federico II dosimeters is placed behind the multimaterial tile. Four samples of TLDs and CR39 are present in the unpackaged configuration and are located behind each material to facilitate the alignment between different materials and maximize shielding geometrical factor.
- a control pouch with all dosimeters. This pouch was kept with data cards close to the detectors and moved in the different locations of the station.
- a ground control pouch followed the others in all phases up to launch in Baikonur.

The pouches are rotated every 6 months, with each taxi flight; since the first set of material was launched at the end of December and returned in April the duration was shorter.

6 Survey of the ISS

Data cards, dosimeters and polyethylene shielding necessary for the experiment were sent on board ISS on 21-12-05 with Progress launcher. The detector was switched on 24-12-05 in the Pirs module in the unshielded configuration. A first data sample of 40 hours was downlinked to the ground to verify the correct functioning of the device. Subsequently two long term sessions with and without shielding material (respectively 11 and 15 days) in the Pirs module were performed. In January 2006 the measurement campaign in the Russian Service module was started: up to now the device was located in both cabins and in several locations of the main area. For each position it has been tried (keeping into account all constraints of logistics and observational time) to have a shielded and an unshielded measurement; measurement with different orientations at the same location have also been performed to assess the differences in flux and nuclear abundances due to differen shielding material.

7 Flight Data

In Figure 4 is shown the acquisition event rate as a function of time for a part of the dataset. Flux modulation is due to the geomagnetic shielding, with higher rate at the poles, where the cutoff is lower and lower rate at the equator where the shielding is higher. The highest peaks occur during passage in the South Atlantic Anomaly (SAA), where particle rate increases more than one order of magnitude due to the trapped proton component. Correlating particle flux

with position information it is possible to build an all particle map (see Figure 5) which shows the latitude increase at high latitude due to galactic particles and the SAA peak due to trapped protons.

8 Nuclear Identification Capabilities

A typical cosmic-ray event, in this case a Neon nucleus crossing the device, is shown in Figure 3 (Top). One of the characteristics of Sileye-3 is its independent channel readout which allows acquisition of multi-particle events due to showers initiated with the interaction of primary particles with the hull or the equipment of the ISS: Figure 3 (Bottom) shows a typical event with this topology. To identify nuclei it is necessary to select single tracks crossing the eight planes of the detector (noise is removed from the events). The energy lost E_{loss} in silicon has been normalized to vertical incidence $E_{loss\,norm.}$ according to the formula: $E_{loss\,norm.} = E_{loss} cos(\theta_{inc})$, with θ_{inc} the angle of incidence from the normal of the silicon planes. An additional cut, requiring that the energy released in the first and the last planes does not differ by more than 20%, selects particles of energy $E_{kin} \gtrsim 70\ MeV/n$ (for C growing with Z up to 150 MeV/n for Fe) . Since the average energy loss of nuclei in matter is described by the Bethe Block formula it basically depends from Z^2/β^2, with $\beta = v/c$ and v the velocity of the impinging particle. Given the differential energy spectrum of cosmic rays hitting the detector, the value of β (and thus the energy lost in the detector) of most particles selected with the above mentioned cut is close to 1, with a smaller [3] amount of low energy particles with a lower β, resulting in a higher energy release tail enlarging the sigma of the gaussian peak. This distribution is further spread by the Landau distribution, describing fluctuations of energy loss in matter. Using the calibration obtained in (30) it is possible to determine the charge spectrum for nuclei up to and above Iron, shown in Figure 6, in this case referring to an 11-day acquisition in the unshielded configuration in the Pirs Module. It is then possible to distinguish the peaks from C to Fe, with the even Z nuclei more abundant end evident than the odd, as found in cosmic rays. Nuclear abundances and trigger efficiency in the different configurations is currently being evaluated.

9 Conclusions

In this work we have outlined the primary goals and presented preliminary results of the Altcriss project on board the International Space Station. The

[3] For instance, 84% of Carbon nuclei in cosmic rays have $1/\beta^2 < 1.2$.

data gathered up to now are under analysis and will be useful in the determination of the radiation environment on board the station and the validation of Montecarlo transport codes. These measurements will be compared with those obtained with a large area detector, the Altea facility(31), sent on the ISS on July 2006. Altea will also continue to investigate the LF phenomenon and the study of cosmic ray radiation in space.

10 Acknowledgements

We wish to thank all ESA staff, in particular E. Istasse, H. Stenuit and A. Savchenko for their invaluable support and help in planning and execution of the experiment. Special thanks go also to D. Castagnolo and R. Fortezza of the Usoc Mars Center (Naples).

References

[1] Saganti, P.B., Cucinotta, F.A., Wilson, J.W., Simonsen, L.C., and Zeitlin, C.J.: Radiation climate map for analyzing risks to astronauts on the Mars surface from galactic cosmic rays. Space Science Rev 110, 143-156, 2004.

[2] Zeitlin, C., Cleghorn, T., Cucinotta, F., Saganti, P., Andersen, V., Lee, K., Pinsky, L., Atwell, W., Turner, R., and Badhwar, G: Overview of the Martian radiation environment experiment. Adv Space Res 33, 2204-2210, 2004.

[3] G. Horneck, R. Facius, et al, Humex, Study of the Survivability and Adaptation of Humans to Long-Duration Exploratory Missions, ESA SP-1264.

[4] Cucinotta F.A., Badhwar G., Saganti P., et.al. (2002), Space Radiation Cancer RiskProjections for Exploration Missions, NASA /Technical Paper - 2002-210777.

[5] NASA, *Strategic Program Plan for Space Radiation Research*, NASA, Washington DC (1998). http://spaceresearch.nasa.gov/docs/radiation_strat_plan_1998.pdf

[6] Reitz G., Beaujean R, Heilmann C et al.,Dosimetry on the Spacelab missions IML1 and IML2, and D2 and on MIR, Rad. Meas, 26, 979-86 (1996)

[7] Sakaguchi T. et al, LET distribution measurement with a new real-time radiation monitoring device-III onboard the Space Shuttle STS-84, NIM A 437, 75-87 (1999)

[8] Badhwar G.D., Shurshakov V.A., Tsetlin V.V., Solar modulation of dose rate onboard the Mir station , IEEE Trans. on Nuc. Science 44(6), 2529-41 (1997)

[9] Badhwar, G.D., Cucinotta, F. A., Depth Dependance of Absorbed Dose, Dose Equivalent and Linear Energy Transfer Spectra of Galactic and

Trapped Particles in Polyethylene and Comparison with Calculations of Models , Rad. Res. 149, 209-18, 1998.
[10] Yasuda H, Badhwar G.D., Komiyama T, Fujitaka K., Effective dose equivalent on the ninth Shuttle-Mir mission (STS-91), Rad. Res. 154(6), 705-13 (2000)
[11] Beaujean R., Kopp J., Reitz G., Active dosimetry on recent space flights, Rad Prot Dosim 85(1-4 Pt2), 223-6 (1999)
[12] Badhwar G.D., Radiation measurements on the International Space Station, Phys. Medica XVII, Suppl. 1, 287-91 (2001)
[13] Reitz G.D., European dosimetry activities for the ISS, Phys. Medica XVII, Supp. 1, 283-6 (2001)
[14] Pinsky L.S., Wilson T.L., Ferrari A., Sala P., Carminati F., Brun R., Development of a space radiation Monte Carlo computer simulation based on the FLUKA and ROOT codes. Phys Med. 2001;17 Suppl 1:86-9.
[15] Wilson, J.; Cucinotta, F.; Golightly, M.; Nealy, J.; DeAngelis, G.; Anderson, B.; Clowdsley, M.; Luetke, N.; Zapp, N.; Shavers, M. International Space Station: A testbed for experimental and Computational dosimetry, proc. of Cospar 2004, session F2.6
[16] K. Niita, T. Sato, H. Iwase, H. Nakashima, and L. Sihver, "Particle and Heavy Ion Transport code System; PHITS", 3rd International Workshop on Space Radiation Research and 15the Annual NASA Space Radiation Health Investigators' Workshop", May 16-20, 204, Danfords on the Sound, Port Jefferson, New York, USA.
[17] T. Ersmark, P. Carlson, E. Daly, C. Fuglesang, et al, "Status of the DESIRE Project: Geant4 Physics Validation Studies and First Results From Columbus/ISS Radiaton Simulations"; IEEE Trans. Nucl. Sci. Vol. 51, p. 1378 (2004).
[18] Cucinotta, F., Durante M., Cancer risk from exposure to galactic cosmic rays: implications for space exploration by human beings, Lancet Oncol 7, 43135 (2006)
[19] Durante M., Biological effects of cosmic radiation in low-Earth orbit, Int. J. Mod. Phys A, 17, 1713-21 (2001).
[20] Durante M., Bonassi S., George K., Cucinotta F.A., Risk estimation based on chromosomal aberrations induced by radiation, Radiat. Reas. **156**, 662 (2001)
[21] Avdeev S., Bidoli V., Casolino M. et al, Eye light flashes on the Mir space station, Acta Astronautica, 50(8), 511-25 (2002).
[22] Bidoli V., Casolino M., De Grandis E. et. al, In-flight performance of SilEye-2 experiment and cosmic ray abundances inside the Mir space station, J. Phys. G, 27, 2051-64 (2001)
[23] M. Casolino, Bidoli V., Morselli A. et al, Dual origins of light flashes seen in space, Nature, 422, 680 (2003).
[24] Shea, M., 2001, Proc. XXVII ICRC, Sh1.07, 3401
[25] Adriani O., Ambriola M., Barbarino, G. et. al, The PAMELA experiment on satellite and its capability in cosmic rays measurements, NIM A 478,

114 (2002)
[26] Bonvicini V., Barbiellini G., Boezio M. et. al, The PAMELA experiment in space, NIM A 461, 262 (2001)
[27] Casolino M., Bidoli V., Furano G. et al., The Sileye-3/Alteino experiment on board the International Space Station, Nuc. Phys. B, 113B, 71-8 (2002).
[28] Bidoli V., Casolino M., De Pascale M.P. et al., The Sileye-3/Alteino Experiment for the Study of Light Flashes, Radiation Environment and Astronaut Brain Activity on Board the International Space Station, J. Radiat. Res., 43, S47-S52 (2002).
[29] Casolino M., Bidoli V., Minori M., et al., Detector response and calibration of the cosmic-ray detector of the Sileye-3/Alteino experiment, Adv. Sp. Res., 37, 9, 1691-1696 (2006).
[30] Casolino M., et al, Detector Response and calibration of the cosmic ray detector of the Sileye-3/Alteino experiment, these proceedings.
[31] Zaconte V., Belli F., Bidoli V., Casolino M., et al, ALTEA: Flight Model Calibration at GSI, Adv. in Sp. Res. 37, 9, 1704-1709 (2006).

Electronics Characteristics	
ADC type	16 bit
Pedestal position	$\simeq 5000\ ADC\ ch$
Conversion Factor	3.3 keV/ADC 8.7 eV/(μm ADC)
1 MIP (Minimum Ionizing Protons)	33 ADC ch 108.6 keV (0.286 keV/μm)
Maximum Energy Detectable	1600 MIP $\simeq$ 174 MeV (460 keV μm)

Table 1
Energy range of the detector electronics.

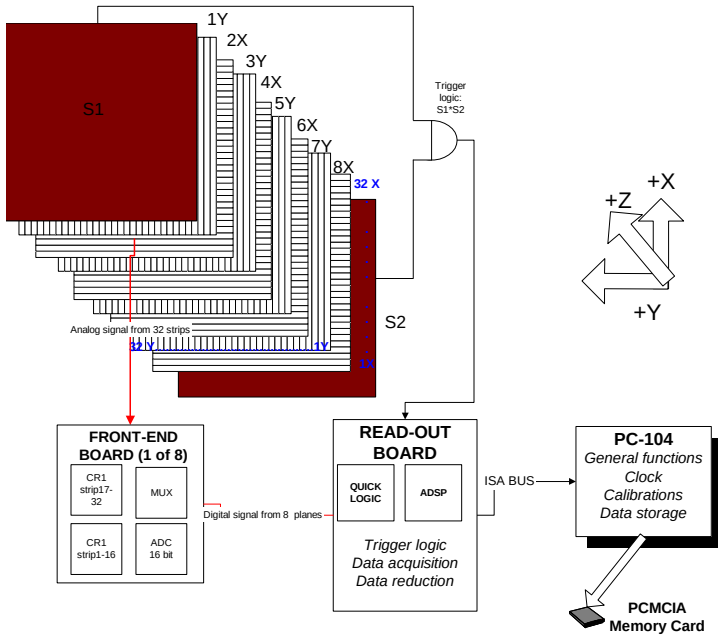

Fig. 1. Scheme of Sileye-3 detector: the 8 silicon planes are triggered by two scintillators (S1*S2), converted on the front end boards (each with 2 CR1.4 preamplifier chip). The signals are read by the DSP board which performs pedestal subtraction and data compression. Data are then sent in blocks of 15kbyte to the PC-104 CPU via ISA bus to be saved on a PCMCIA flash card.

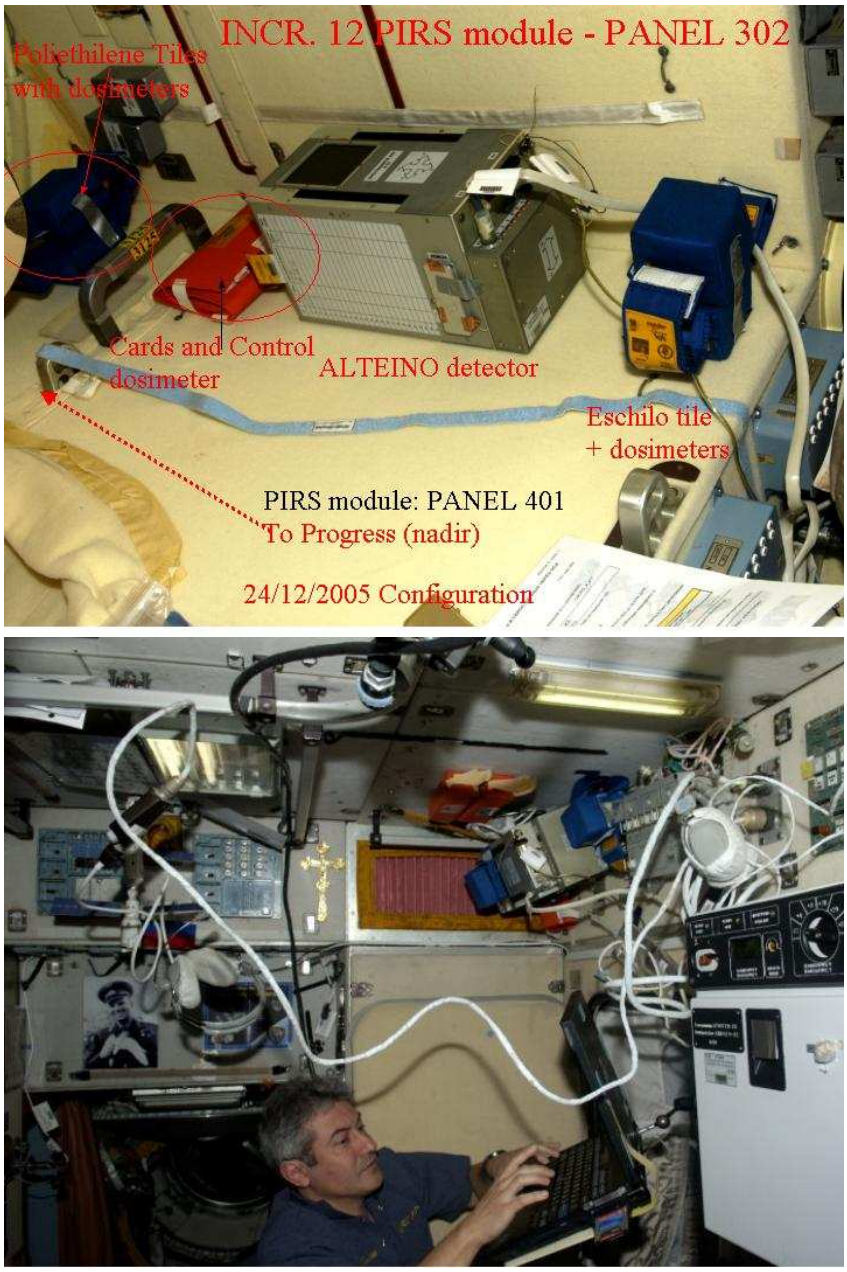

Fig. 2. Top: Sileye-3 in the Pirs module (Panel 302) of the ISS in its first switch on of the Altcriss Survey (24-12-2005). The device is in its unshielded configuration, with the poliethilene shielding tiles on the left of the picture (in the Soyuz / nadir direction) and the multimaterial tiles on the right of the picture (in the direction of the station). Bottom: Sileye-3 the Service Module of the ISS (05-04-2006). The device is located in the shielded configuration on top of the portside crew cabin door (Panel 234). In the foreground it is possible to see Brazilian cosmonaut Marcos Pontes.

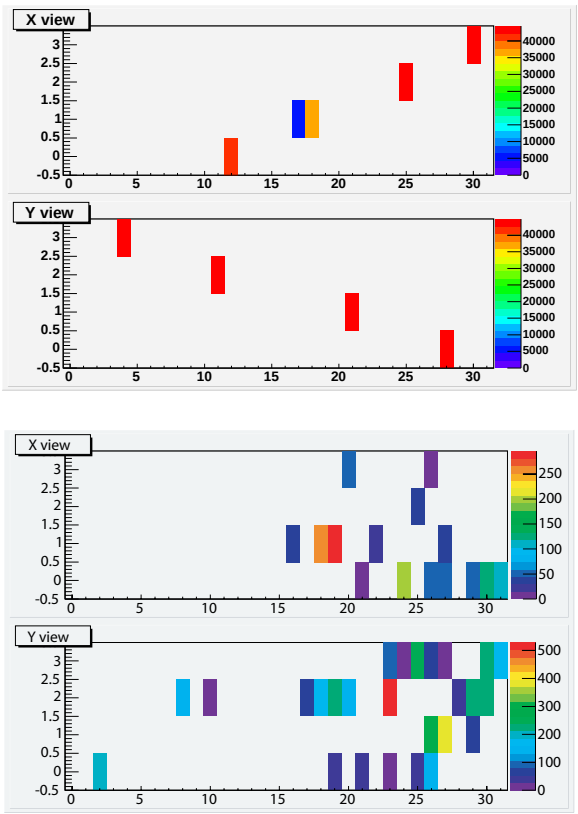

Fig. 3. Typical events obtained with Sileye-3. Top: A Neon nucleus. Bottom: A shower event crossing the detector. Top Panel: X view, Bottom Panel Y view. x axis: strip number (1-32), y axis: plane number (1-4).

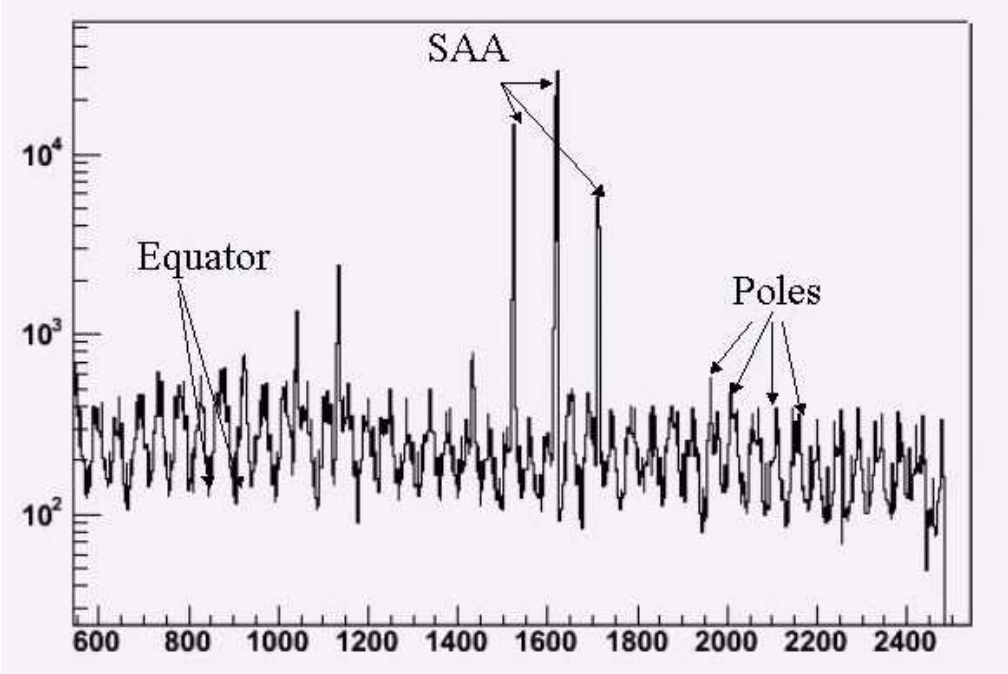

Fig. 4. Cosmic ray flux vs time during one typical acquisition session Note the passage in the SAA (higher peaks) and the modulation due to passage through the equator and the poles.

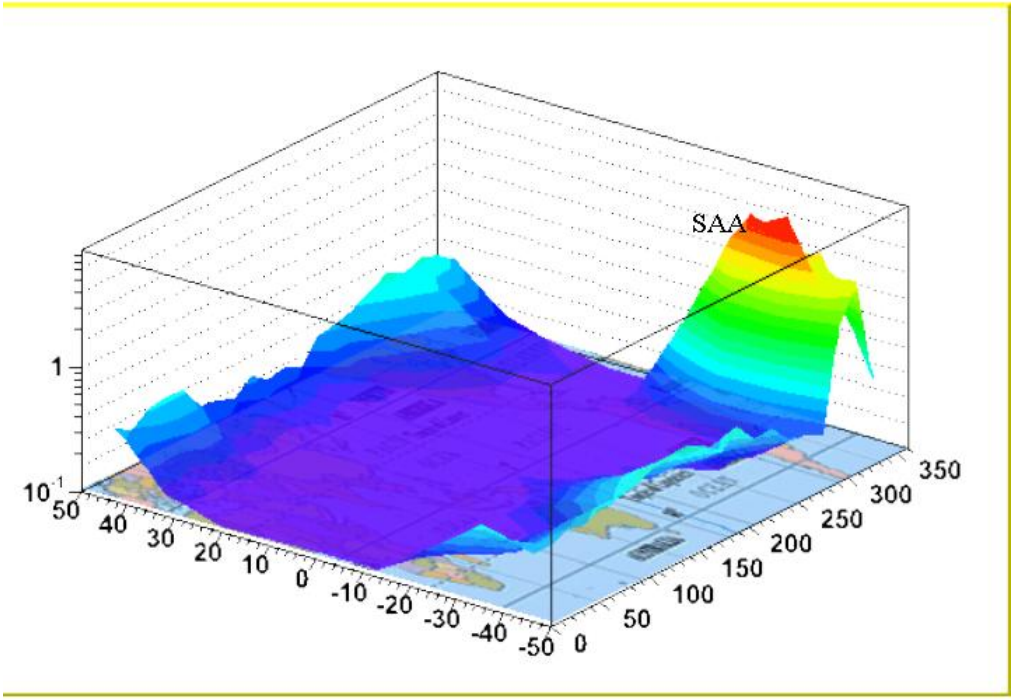

Fig. 5. All particle rate vs position measured with Sileye-3. It is possible to see the trapped proton peak in the South Atlantic Anomaly and the increase in the high latitude regions due to galactic nuclei.

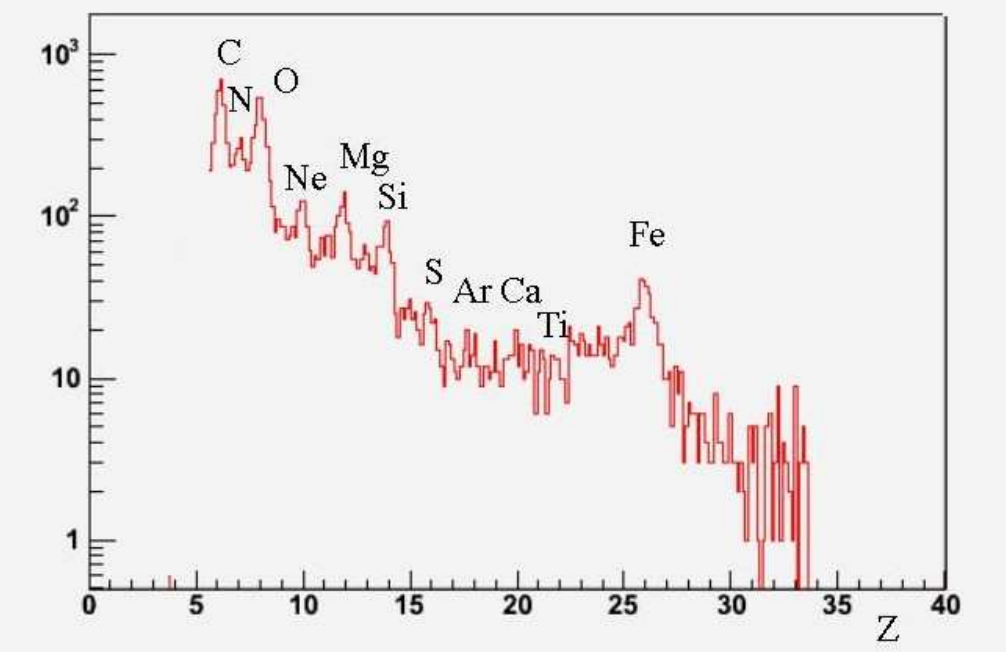

Fig. 6. Nuclear identification capability of Sileye-3 from C to Fe in the Pirs module. Note how even numbered nuclei are more abundant than odd numbered ones.